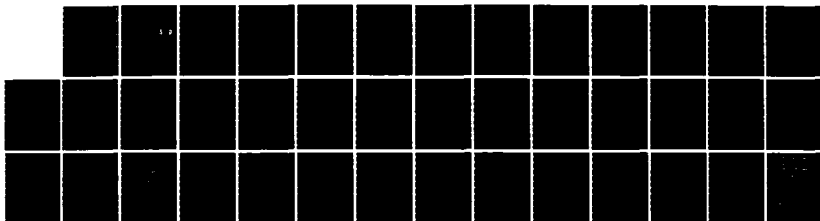
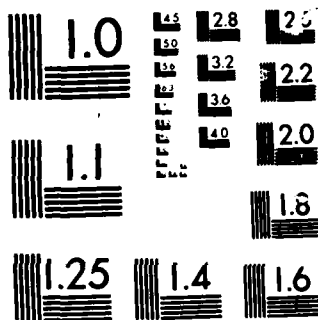


AD-A166 648 ABSORPTION BY H2O IN NARROW WINDOWS BETWEEN 3000 AND 1/1
4200 CM(-1)(U) FORD AEROSPACE AND COMMUNICATIONS CORP
NEWPORT BEACH CA AERON. D E BURCH MAR 85 U-6816
UNCLASSIFIED AFGL-TR-85-0036 F19628-81-C-0118 F/G 7/4 NL





MICROCOPY

CHART

2

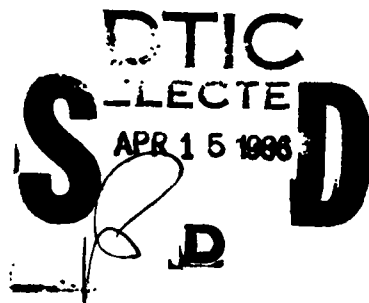
AFGL-TR-85-0036

ABSORPTION BY H_2O IN NARROW WINDOWS BETWEEN 3000 and 4200 CM^{-1}

AD-A166 648

Darrell E. Burch

Ford Aerospace & Communications Corporation
Aeronutronic Division
Ford Road, Newport Beach, CA. 92663



March 1985

Final Report for Period September 1981 - March 1985

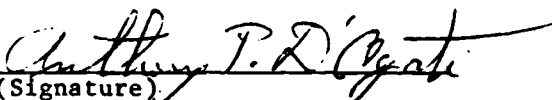
Approved for public release, distribution unlimited

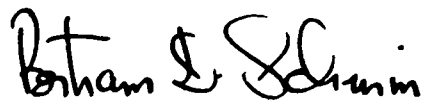
DTIC FILE COPY

AIR FORCE GEOPHYSICS LABORATORY
AIR FORCE SYSTEMS COMMAND
UNITED STATES AIR FORCE
HANSCOM AFB, MASSACHUSETTS 01731

10 4 1 078

"This technical report has been reviewed and is approved for publication"


(Signature)
ANTHONY P. D'AGATI
Contract Manager


(Signature)
BERTRAM D. SCHURIN
Branch Chief

FOR THE COMMANDER


(Signature)
JOHN S. GARING
Division Director

This report has been reviewed by the ESD Public Affairs Office (PA) and is releasable to the National Technical Information Service (NTIS)

Qualified requestors may obtain additional copies from the Defense Technical Information Center. All others should apply to the National Technical Information Service.

If your address has changed, or if you wish to be removed from the mailing list, or if the addressee is no longer employed by your organization, please notify AFGL/DAA, Hanscom AFB, MA 01731. This will assist us in maintaining a current mailing list.

Do not return copies of this report unless contractual obligations or notices on a specific document requires that it be returned.

Unclassified

SECURITY CLASSIFICATION OF THIS PAGE

AD-A166648

REPORT DOCUMENTATION PAGE

1a. REPORT SECURITY CLASSIFICATION Unclassified			1b. RESTRICTIVE MARKINGS	
2a. SECURITY CLASSIFICATION AUTHORITY			3. DISTRIBUTION/AVAILABILITY OF REPORT Approved for public release; distribution unlimited	
2b. DECLASSIFICATION/DOWNGRADING SCHEDULE				
4. PERFORMING ORGANIZATION REPORT NUMBER(S) U6816 ✓			5. MONITORING ORGANIZATION REPORT NUMBER(S) AFGL-TR-85-0036	
6a. NAME OF PERFORMING ORGANIZATION Ford Aerospace and Communications Corporation		6b. OFFICE SYMBOL (If applicable)	7a. NAME OF MONITORING ORGANIZATION Air Force Geophysics Laboratory	
6c. ADDRESS (City, State, and ZIP Code) Newport Beach, CA 92667			7b. ADDRESS (City, State, and ZIP Code) Hanscom AFB, Massachusetts 01731	
8a. NAME OF FUNDING/SPONSORING ORGANIZATION Air Force Geophysics Laboratory		8b. OFFICE SYMBOL (If applicable)	9. PROCUREMENT INSTRUMENT IDENTIFICATION NUMBER F19628-81-C-0118	
8c. ADDRESS (City, State, and ZIP Code) Hanscom AFB, Massachusetts 01731			10. SOURCE OF FUNDING NUMBERS	
			PROGRAM ELEMENT NO 62101F	PROJECT NO 7670
			TASK NO. 09	WORK UNIT ACCESSION NO AP
11. TITLE (Include Security Classification) (U) Absorption by H ₂ O in Narrow Windows between 3000 and 4200 cm ⁻¹				
12. PERSONAL AUTHOR(S) Darrell E. Burch				
13a. TYPE OF REPORT Final		13b. TIME COVERED FROM Sept '81 to Mar '85	14. DATE OF REPORT (Year, Month, Day) 1985, March	
15. PAGE COUNT 38				
16. SUPPLEMENTARY NOTATION				
17. COSATI CODES			18. SUBJECT TERMS (Continue on reverse if necessary and identify by block number)	
FIELD	GROUP	SUB-GROUP		
			H ₂ O Continuum Absorption, Atmospheric Transmission; Line Shape Absorption; water vapor	
19. ABSTRACT (Continue on reverse if necessary and identify by block number)				
<p>The measured H₂O absorption in narrow windows between strong lines in the 3000-4200/cm⁻¹ region is consistently greater than that calculated by using standard theoretical line shapes and well-established values of the positions, strengths and widths of the lines. The difference between the experimental and calculated coefficients is called the empirical continuum because it appears to change gradually with changing wavenumber. This extra absorption is attributed to deviations of the shapes of the wings of the collision-broadened absorption lines from the theoretical shapes. Self-broadened lines, from pure H₂O samples, display greater deviations than N₂ broadened lines from the theoretical shape. The results are consistent with our previous results in the 1300-2200/cm⁻¹ region.</p>				
20. DISTRIBUTION/AVAILABILITY OF ABSTRACT <input checked="" type="checkbox"/> UNCLASSIFIED/UNLIMITED <input checked="" type="checkbox"/> SAME AS RPT. <input type="checkbox"/> DTIC USERS			21. ABSTRACT SECURITY CLASSIFICATION Unclassified	
22a. NAME OF RESPONSIBLE INDIVIDUAL Anthony D'Agati			22b. TELEPHONE (Include Area Code) 617-861-4776	22c. OFFICE SYMBOL OPI

DD FORM 1473, 84 MAR

83 APR edition may be used until exhausted
All other editions are obsolete

SECURITY CLASSIFICATION OF THIS PAGE

CONTENTS

<u>SECTION</u>	<u>PAGE</u>
1. INTRODUCTION.....	5
Background and Summary.....	5
Definitions, Symbols and Parameters.....	6
2. EXPERIMENTAL.....	10
Sampling.....	10
Transmission Measurements.....	11
3. RESULTS AND DISCUSSION.....	12
Calculations and Data Reduction.....	12
Self Broadening: 3000 - 4200 cm^{-1}	17
N ₂ Broadening: 3000 - 4000 cm^{-1}	25
Empirical Continuum: 1300 - 2200 cm^{-1}	27
Spectral Band Contours of Liquid Vapor and Empirical Continuum.....	32
4. PREVIOUS REPORT AND PAPERS UNDER PRESENT CONTRACT.	36
5. REFERENCES.....	37

Accession For	
NTIS CRA&I	<input checked="" type="checkbox"/>
DTIC TAB	<input type="checkbox"/>
Unannounced	<input type="checkbox"/>
Justification	
By	
Distribution /	
Availability Codes	
Dist	Avail and/or Special
A-1	



LIST OF FIGURES

<u>Figure</u>		<u>Page</u>
1	Spectral plots of transmittance in two narrow windows near 3987.30 and 3072.0 cm^{-1}	13
2	Spectral plots of transmittance in three narrow windows near 3682.78, 3717.32, and 3729.62 cm^{-1}	14
3	Spectral plots of the normalized absorption coefficients from 3000 to 4200 cm^{-1} for self broadening.....	18
4	Corrected absorption coefficients for self broadening compared with coefficients calculated from FASCODE.....	24
5a	Spectral plots of the normalized absorption coefficients from 3000 to 4200 cm^{-1} for N_2 broadening.....	26
5b	Corrected absorption coefficients for N_2 broadening compared with coefficients calculated from FASCODE.....	28
6	Spectral plots of the normalized absorption coefficients from 1400 to 1800 cm^{-1} for pure H_2O	31
7	Composite of spectral curves of the empirical continuum from 1300 to 2200 cm^{-1} at various temperatures.....	32
8	Comparison of the spectral curves between 3000 and 4200 cm^{-1} of the empirical continuum for self broadening, the absorption coefficient of liquid water, and the average intensities of the H_2O vapor lines.....	34
9	Comparison of the spectral curves between 1350 and 1850 cm^{-1} of the empirical continuum for self broadening, the absorption coefficient of liquid water, and the average intensities of the H_2O vapor lines.....	35

SECTION I

INTRODUCTION

BACKGROUND AND SUMMARY

Theoretically derived shapes of collision-broadened H_2O lines have been well verified in regions within a few cm^{-1} of the line centers. However, it is well known¹⁻³ that the absorption by the extreme wings of the lines cannot be accurately calculated solely on the basis of the known line parameters: position, intensity and width. The atmospheric windows centered near 1000 cm^{-1} and 2600 cm^{-1} are two examples of spectral regions where H_2O absorption is quite different from that calculated from theoretical shapes. A major reason for the disagreements with the absorption theory is the lack of understanding of the shapes of the extreme wings of the absorption lines. Measurements of the weak absorption in the major windows show that the extreme wings of the lines deviate significantly from the theoretical shapes beyond approximately 50 cm^{-1} from the line centers.

In a previous report¹, we have shown evidence that the actual shapes of the H_2O lines also deviate from theoretical at closer distances from the line centers, probably as close as 5 or 10 cm^{-1} . Most workers in this field had previously assumed that the theoretical shapes were still correct at greater distances than this from the centers. The previous report¹ that indicates deviation from theoretical shapes in the intermediate wings deals with absorption in several narrow windows between the strong lines centered from approximately 1300 cm^{-1} to 2000 cm^{-1} . The present report summarizes a similar study of approximately 50 narrow windows between strong lines from 3000 cm^{-1} to 4200 cm^{-1} .

The general results of the present work are consistent with those of the similar study in a different vibration-rotation band. In all of the narrow windows within the main parts of the bands, the observed absorption is greater than that predicted from the Lorentz line shape and the AFGL⁴ parameters. The relative difference between experimental and theoretical results is greater for self broadening than for N_2 broadening. This relative difference is also greater in regions where most of the absorption is due to lines centered more than 10 cm^{-1} away than it is in regions very near the strong lines.

1. D. E. Burch, AFGL-TR-81-0300, ADA112264, Final Report, AFGL Contract No. F19628-79-0041 (1982).
2. D. E. Burch and D. A. Gryvnak, Continuum Absorption by H_2O Vapor in Atmospheric Water Vapor (A. Deepak, T. D. Wilkerson, and L. H. Ruhnke, eds), Academic Press, New York (1980).
3. D. E. Burch, SPIE Proceedings 277, 28 (1981).
4. R. A. McClatchey, W. S. Benedict, S. A. Clough, D. E. Burch, R. F. Calfee, K. Fox, L. S. Rothman, and J. S. Garing, AFCRL Atmospheric Absorption Line Parameters Compilation, AFCRL-TR-73-0096, U. S. Air Force (1973). (Available from NTIS), AD762904.

We attribute the "excess" absorption at the wavenumbers of minimum absorption to a super-Lorentzian line shape beyond about 5 or 10 cm^{-1} from the line centers. It cannot be due entirely to errors in the assumed intensities or widths of the lines. Errors of this type would cause deviations between the theoretical and experimental results at positions close to the strong lines. Such errors were not observed.

The excess absorption, which we call empirical continuum, does not exhibit rapid variations with changing wavenumber throughout the band, but it is greatest in regions that contain the strongest lines. It is too small to be checked very near the strong lines, where the absorption is dominated by the lines themselves. Thus, ignoring the empirical continuum in a line-by-line calculation leads to significant errors only in the windows a few cm^{-1} from the lines producing most of the absorption. The average transmittance over wide spectral intervals is not strongly dependent upon the empirical continuum when the average transmittance is high. But the errors in calculated average transmittance may be large for long paths over which the only significant transmittance is in the windows where the empirical continuum plays a major role.

DEFINITIONS, SYMBOLS AND PARAMETERS

At pressures corresponding to the lower atmosphere, the vibration-rotation lines of infrared H_2O vapor are collision broadened. It has been well established that the shape of one of these lines within a few cm^{-1} of its center is given by the simple Lorentz equation.

$$k = \frac{S}{\pi} \frac{\alpha}{(\nu - \nu_0)^2 + \alpha^2}, \text{ (simple Lorentz)} \quad (1)$$

where k is the absorption coefficient at wavenumber ν , and ν_0 is the line center. It has also been well established that the line intensity S is essentially independent of the half width α , which is proportional to pressure. For a line shape to be exact, the line intensity S must be related to k by

$$S = \int_0^\infty k \, d\nu. \quad (2)$$

The simple Lorentz shape given by Equation (1) is known to be invalid in the far infrared and millimeter regions, or in the extreme wings of any lines where $|\nu - \nu_0|$ is no longer much less than α . References 5 and 6 discuss more appropriate theoretical shapes for all spectral regions and their deviations from experimental results. No line shape derived strictly on theoretical considerations agrees with experimental results in all of the spectral regions from the visible to the microwaves.

5. S. A. Clough, F. X. Kneizys, R. Davies, R. Gamache, and R. Tipping, Theoretical Line Shape for H_2O Vapor: Application to Continuum, in Atmospheric Water Vapor (A. Deepak, T. D. Wilkerson, and L. H. Ruhnke, eds.), Academic Press, New York (1980).
6. S. A. Clough, F. X. Kneizys, L. S. Rothman, and W. O. Gallery, SPIE Proceedings 277 (1981).

This report presents new data on H₂O vapor absorption between approximately 3000 cm⁻¹ and 4200 cm⁻¹, and compares the results with a previous similar study of the 1250-2200 cm⁻¹ region. Essentially none of the absorption in either of these intervals is due to lines centered outside of the interval. In calculating the absorption within this region, the results obtained by summing the contributions by lines with the Lorentz shape are very nearly the same as those obtained by using the more complex form developed in References 5 and 6. Therefore, for simplicity, we have chosen to use the more common, simple Lorentz form for calculations to compare with experimental results.

The emphasis in this report is on the absorption in approximately 50 very narrow windows between the lines. At the wavenumbers selected for study, very little of the absorption is due to an absorption line centered closer than 1 cm⁻¹. In every case, the measured absorption is greater than that predicted by summing the calculated contributions by the lines. The excess absorption is the main subject of this study.

The absorption coefficient for a single line is related to the true transmittance T' of the line that would be observed with infinite resolving power (zero slit width) by:

$$k = (-1/u) \ln T' \quad (3)$$

The absorber thickness u is given by:

$$u(\text{molecules cm}^{-2}) = p(\text{atm}) \cdot 7.34 \times 10^{21} L(\text{cm})/\theta \quad (4)$$

where θ is the temperature in Kelvin. L is the geometrical path length of the radiation through the sample consisting of H₂O vapor at partial pressure p. It follows that the units for S, defined by Equation (2), are molecules⁻¹ cm² cm⁻¹.

The absorption coefficient given by any theoretical shape for collision-broadened lines is proportional to α in the extreme wings where $\nu - \nu_0 \gg \alpha$. This proportionality relationship appears experimentally to be valid, even when the coefficient is greatly different from that given by any of the theoretical expressions. The halfwidth of a collision-broadened line for a mixture of H₂O in N₂ at a fixed temperature is given by:

$$\alpha = \alpha_S^0 p + \alpha_N^0 p_N \quad (5)$$

The partial pressures in atmospheres of the H₂O and N₂ are represented by p and p_N, respectively. N₂ is used to simulate dry air. Both α_S^0 and α_N^0 are assumed to be proportional to $\theta^{-0.62}$, as recommended by Reference 4 for H₂O lines. The equivalent pressure p_e is proportional to regardless of the relative values of p and p_N.

$$p_e = Bp + p_N = (B-1)p + P \quad (6)$$

where P is the total pressure, and

$$B = \alpha_S^0 / \alpha_N^0 \quad (7)$$

B for H₂O has been determined experimentally to be approximately 5; this value is used in all of our calculations reported here.

The total absorption coefficient K at a given wavenumber due to many lines is

$$K = \sum_i k_i = (-1/u) \ln T', \quad (8)$$

where each k_i represents the coefficient due to an individual line, u is given by Equation (4), and T' is the true transmittance that would be observed with infinite resolving power (zero spectral slit width). The present work deals with collision-broadened lines, each of which can conveniently be treated as having two regions, one near the center and one in the wings. Thus, we write K, the total absorption coefficient, as

$$K = -(1/u) \ln T' = K(\text{local}) + K(\text{wing}) \quad (9)$$

At any wavenumber, $K(\text{local})$ represents the contribution due to nearby lines for which $|v-v_0|$ is not large compared to α . $K(\text{wing})$ is then defined as the contribution due to the wings of lines for which $|v-v_0| \gg \alpha$. The present effort deals with selected wavenumbers at which $K(\text{local})$ is much less than $K(\text{wing})$. This makes it possible to make quantitative comparisons between the experimental and calculated values of $K(\text{wing})$. As discussed above, the main purpose of this study is to compare the experimentally observed wing absorption with that calculated by using the simple Lorentz line shape given by Equation (1). The $K(\text{local})$ portion of the absorption is small, but significant, and is assumed to be given accurately by the simple Lorentz line shape. The method of accounting for the $K(\text{local})$ contribution is explained in Section 3.

All of the experimental values of window absorption measured during the present study are greater than the corresponding calculated values. We define the difference, or "extra absorption", as an empirical continuum:

$$e_c = K(\text{exp}) - K(\text{calc}). \quad (10)$$

Because of the assumption that the $K(\text{local})$ contributions to the absorption are accounted for, the empirical continuum is equivalent to the differences in wing absorption: $K(\text{wing, exp}) - K(\text{wing, calc})$. The results indicate that the extra absorption as defined by the above equations does not vary rapidly over spectral intervals a few cm^{-1} wide; therefore, the word continuum is appropriate.

In a sample of pure H₂O vapor with no other gas present, all of the line broadening is due to collisions of the absorbing H₂O molecules with other H₂O molecules. Such H₂O-H₂O collisions lead to self broadening. In samples of H₂O + N₂, both self broadening and N₂ broadening of the H₂O lines take place, and each contributes to the $K(\text{wing})$ coefficient.

From Equation (1) we see that k , the coefficient due to a single line, is proportional to α in the wings where $|v-v_0| \gg \alpha$. Thus, $K(\text{wing})$, which is due to the contributions by the wings of all the lines, is made up of two components, one proportional to p and one proportional to pN . We define two normalized empirical continuum coefficients e_{c0}

and $e_{N_2}^0$ that represent self broadening and N_2 broadening, respectively. The superscript 0 represents a normalization to 1 atm pressure of H_2O vapor or N_2 . Subscripts s and N denote self broadening and N_2 broadening, respectively.

For self broadening only,

$$p(\text{atm}) \tau_s^0 = \tau_s = K_s(\text{exp}) - K_s(\text{calc}). \quad (11)$$

$K_s(\text{calc})$ is determined by summing the contributions of all of the lines with the following assumptions: that the line shapes are given by Equation (1); S , ν_0 , and α_N^0 are the values given by the AFGL line parameters compilation(4); and $\alpha_s^0 = 5\alpha_N^0 p(\text{atm})$, in accordance with Equations 5 and 7.

For a mixture of $H_2O + N_2$,

$$e_c = e_{c_s} + e_{c_N} = p e_{c_s}^0 + p_N e_{c_N}^0 \quad (12)$$

$$\text{where } e_{c_N} = K_N(\text{exp}) - K_N(\text{calc}). \quad (13)$$

$K_N(\text{calc})$ is determined by summing the contributions of all of the lines by the same method used to calculate $K_s(\text{calc})$, except that the value used for half width is α_N .

The above definitions of transmittance T' , k , K , and e_c correspond to a single wavenumber; i.e., to measurements that would be made with infinite resolving power. The spectrometer used in the measurements passes a finite spectral interval, typically between 0.5 and 1 cm^{-1} ; thus the observed transmittance $T(\text{exp})$ differs from the true transmittance T' . The method described in Section 3 to account for the finite spectral slitwidth involves calculations of $T'(\text{calc})$ and $T(\text{calc})$. At a fixed wavenumber, $T'(\text{calc})$ for a given value of u is calculated by use of Equation (8). Values of $T'(\text{calc})$ are calculated at many wavenumbers with the intervals between points of calculation small enough that the spectral structure is retained. These values of $T'(\text{calc})$ are then convolved with a slit function similar to the known experimental slit function to determine values of $T(\text{calc})$. These values of $T(\text{calc})$ are compared to values of $T(\text{exp})$ to determine the deviation of the theoretical results from the experimental results. This procedure is illustrated with typical spectra in the discussion of data reduction in Section 3.

After determining the continuum coefficient at each wavenumber studied, we used its value to find the corrected value for the total absorption coefficient. We then compared these corrected values to corresponding values calculated by Air Force Geophysics Laboratory scientists using the well known FASCODE⁶ computer program.

SECTION 2

EXPERIMENTAL

The experimental methods are similar to those we have used for several investigations of absorption by H_2O and other atmospheric gases. Gas samples are contained in either of two multiple-pass absorption cells that provide optical paths from approximately 2 meters to 1000 meters. Spectral transmittances are measured with a grating spectrometer mounted in a tank that can be evacuated to avoid absorption by atmospheric gases in the optical path outside of the sample cell.

SAMPLING

All of the new data reported here have been obtained with samples of either pure H_2O vapor or of $H_2O + N_2$ at room temperature, 296K. The typical sampling procedures are as follows:

The cell is evacuated to less than 0.1 torr immediately before H_2O vapor is added. Distilled liquid water is contained in a small "boiler" attached to the sample cell by a short piece of tubing with a valve. The tubing is connected to the liquid container above the liquid level so that only the vapor can pass through the tubing to the cell. After the valve is opened to allow H_2O vapor to enter the cell, the liquid is heated to speed up the evaporation and the transfer of vapor from the container to the sample cell. Approximately 10-15 minutes is normally required to add H_2O to a pressure of 15 torr (approximately 0.02 atm). The pressure is allowed to stabilize before spectral measurements are made.

Another tube with a valve connects the upper portion of the liquid container to a vacuum pump that removes any air from the container before the valve is opened in the tubing to the sample cell. The tubing to the pump and sample cell are electrically heated to avoid condensation in them.

Sample pressures below approximately 0.1 atm are measured with an oil manometer; pressures from 0.1 atm to 2 atm are measured with a mercury manometer. A Dubrovin gauge serves for pressures between 2 atm and 15 atm. The manometers and gauge are at room temperature, making it necessary to use extra care to avoid condensation in them while studying samples at pressures above the H_2O vapor pressure at room temperature. Normally, the manometer or gauge and the tubing connecting them to the sample cell are filled with dry N_2 to a pressure slightly above the sample pressure; the valve is then opened, allowing a small amount of dry N_2 to flow into the cell until the pressure comes to equilibrium. Because of the very large volume of the sample cell, the small amount of dry N_2 entering from the manometer line makes a trivial change in the sample pressure.

Samples of $H_2O + N_2$ are made by first adding the H_2O to the evacuated cell and allowing the pressure to come to equilibrium. If the H_2O is added and allowed to remain, the pressure decreases by 20-30% during the first 24 hours and may continue to decrease slowly for another 1 or 2 days because of the slow absorption of H_2O on the walls of the cell. The H_2O pressure is normally brought to near equilibrium much

more quickly by first adding H_2O to a pressure 10-20% higher than the desired equilibrium pressure. The gas is allowed to remain for several minutes, then part of it is pumped out until the pressure is approximately equal to the desired equilibrium pressure. If this sample is allowed to remain, the pressure does not normally change more than a few percent during the next several hours. The pressure of a pure H_2O sample is measured again at the time of a transmittance measurement.

Dry N_2 from commercial cylinders is slowly added to the H_2O in the sample cell through 4 different ports distributed evenly along the length of the cell. While the N_2 is entering the cell, mixing fans inside the cell are turned on periodically to ensure good mixing. Immediately before the spectral data for the $H_2O + N_2$ sample are obtained, the H_2O partial pressure is measured with a dewpoint meter inside the sample cell. The results are compared with the H_2O pressure measurements made before adding the N_2 : one with the dewpoint meter and one with the manometer. The dewpoint is measured periodically while a sample of $H_2O + N_2$ is in the cell to monitor the H_2O partial pressure. Any small changes that occur are accounted for during the data reduction.

Possible errors in transmission measurements due to adsorption of water on the optical surfaces in the longer cell are greatly reduced by heating the windows and the internal mirrors to approximately 3 K above the gas temperature. Transmission measurements made with pure non-absorbing N_2 indicate that there is negligible effect due to any turbulence or temperature non-uniformities caused by the heated optical components.

TRANSMISSION MEASUREMENTS

Infrared radiation from a Nernst glower is chopped and directed through a window into the multiple-pass absorption cell that contains the sample to be studied. After the beam of energy has passed back and forth the desired number of times in the cell, it is directed out through an exit window to a grating spectrometer.

The spectrometer is used either to scan a portion of the spectrum of interest or to remain set so it will pass only a narrow spectral interval at one of the wavenumbers where the continuum absorption is being measured. These narrow intervals are chosen between H_2O absorption lines where there is little interference by nearby lines in the continuum measurement.

The transmittance of a sample is determined by comparing the level of the infrared signal measured with the sample in the cell to that measured when the cell is evacuated. The background spectrum, or background signal level at a few specific wavenumbers, is typically obtained before and after the measurement on the gas sample. The number of passes of the sample cell can be changed without disturbing the sample, making it possible to investigate samples of different absorber thickness from a single batch of gas. When this procedure is followed, background data are obtained with the evacuated cell at all of the same path lengths used for the samples.

SECTION 3

RESULTS AND DISCUSSION

Experimental data presented in this section for the 3000-4200 cm^{-1} region are from two sources. The data on self broadening have been obtained recently under the present contract, whereas those data on N_2 broadening are from one of our previous reports⁷. The analysis of the data is similar to that used previously by us¹⁻³ for data obtained in narrow windows of the strong H_2O band between 1250-2200 cm^{-1} . Some of the results of the previous study are repeated in this section for comparison with the new data.

CALCULATIONS AND DATA REDUCTION

Figures 1 and 2 illustrate the method used to compare the experimental results with theoretical results to determine the empirical continuum in each of the narrow windows. The solid curve in each panel is based on calculations for a sample with the indicated equivalent pressure and absorber thickness to match an experimental sample. Values of the true transmittance $T'(\text{calc})$ for the solid curve were calculated according to Equation (8) at 0.02 cm^{-1} intervals by summing the calculated contributions by all of the lines centered between 2900 cm^{-1} and 4200 cm^{-1} . Intensities, widths and positions of the lines used in the computations are from the 1982 version of the AFGL⁴ line parameter tapes.

The upper panel of Figure 1 covers a narrow spectral interval on the low-wavenumber side of the region studied. All of the strong absorption lines are centered at higher wavenumbers, and most of the absorption displayed in the narrow interval between 3071.5 and 3072.5 cm^{-1} is due to the extreme wings of these lines. Only a very small fraction of the absorption in this interval is due to the two weak lines centered near 3071.3 and 3072.8 cm^{-1} . The short curve made up of long dashes in the upper panel of Figure 1 is from the experimental spectrum obtained for a laboratory sample with the same parameters as those used for the calculated spectrum. Because of the finite slitwidth of the spectrometer used to obtain the data, the experimental curve is smoothed and does not show much of the structure found in the calculated spectrum of $T'(\text{calc})$. In order to make a more direct comparison between the experimental data and theoretical results, we computed the degraded spectrum of $T(\text{calc})$, represented by the curve of short dashes, by convolving the calculated true transmittance spectrum with a spectral slitwidth $\text{SW} = 0.6 \text{ cm}^{-1}$ to match the spectral slitwidth of the spectrometer. The form of the triangular slit function is illustrated in the lower panel of Figure 1. The appropriate slitwidth, which varied from approximately 0.6 cm^{-1} near 3000 cm^{-1} to 1 cm^{-1} near 4200 cm^{-1} , was used for each calculation of $T(\text{calc})$.

7. D. E. Burch, D. A. Gryvnak, and R. R. Patty, Scientific Report, Contract NOnr 3560(00), ARPA Order No. 273/11-7-63 (1965)

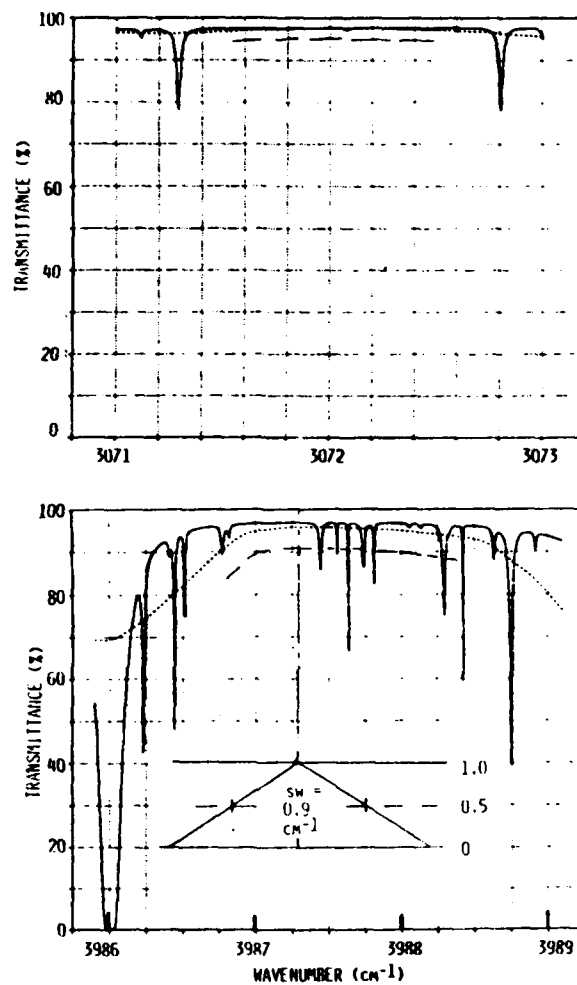


Figure 1: Spectral plots of transmittance in two narrow windows near 3987.30 and 3072.0 cm^{-1} . Solid curve, calculated true transmittance; short-dashed curve, calculated transmittance with slit function; long-dashed curve, experimental. Upper panel: $u = 4.72 \times 10^{22}$ molecules cm^{-2} , $p = 0.0226$ atm. Lower panel: $u = 1.37 \times 10^{22}$ molecules cm^{-2} , $p = 0.0226$ atm.

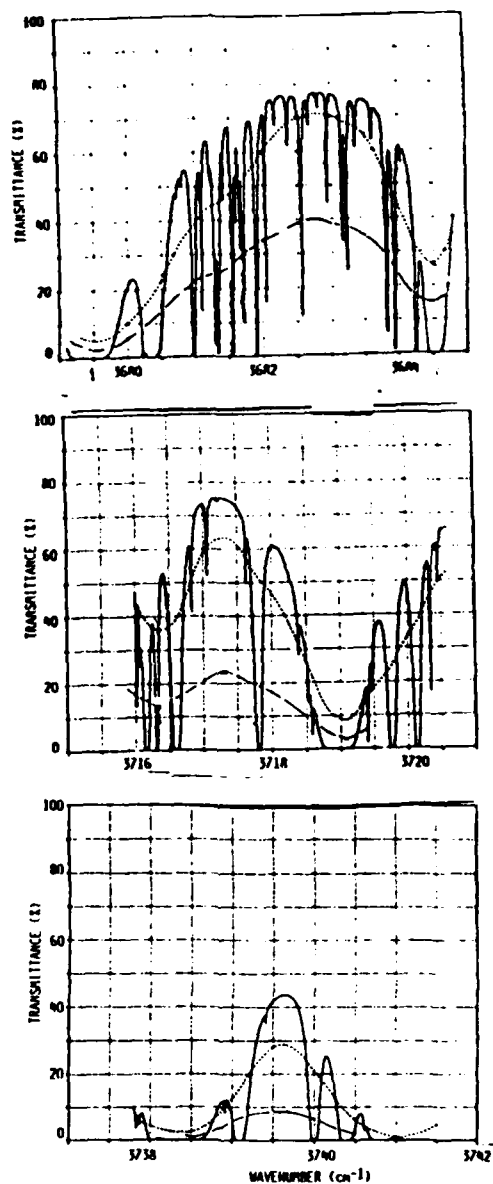


Figure 2: Spectral plots of transmittance in three narrow windows near 3682.78, 3717.32, and 3739.62 cm^{-1} . Solid curve, calculated true transmittance; short-dashed curve, calculated transmittance with slit function; long-dashed curve, experimental. $u = 3.66 \times 10^{21}$ molecules cm^{-2} , $p = 0.0226$ atm for all three panels.

The curves in the lower panel of Figure 1 represent a narrow window on the high wavenumber side of the many very strong lines in the strong band covered in this study. As in the upper panel, much of the calculated absorption at the wavenumbers of maximum transmittance between the very weak lines is due to the extreme wings of distant lines. Also, as in all of the 50 narrow windows investigated, the experimental transmittance near the center of the window is less than that calculated on the basis of the known line intensities and widths. Within each window, the excess absorption has the nature of a continuum, i.e., it does not show the structure associated with lines. Thus, we call it the empirical continuum because it provides an empirical fit between the theoretical results and the experimental data.

The value of the normalized empirical coefficient, eC_s for self broadening near the center of a window, is determined by comparing the experimental value $T(\text{exp})$ near the wavenumber of maximum transmittance with the corresponding calculated transmittance $T(\text{calc})$, which includes convolution of the slit function.

$$T(\text{emp}) = T(\text{exp}) / T(\text{calc}), \text{ and} \quad (14)$$

$$eC_s = (-1/u_p) (\ln T(\text{emp})) \quad (15)$$

A similar method is used to determine the empirical continuum coefficients for N_2 broadening. Samples of $H_2O + N_2$ used for this part of the study were at total pressures of either 5 atm or 10 atm with the H_2O partial pressure p less than 0.03 atm. Thus, the self broadening is much less than the N_2 broadening for these samples, and can be ignored when comparing the experimental transmittance to the calculated $T(\text{calc})$. It follows that the corresponding coefficient for N_2 broadening is:

$$eC_N = (-1/u_{p_N}) (\ln T(\text{emp})) \quad (16)$$

This method of comparing experimental results with the calculated values accounts for the effects of the finite slitwidth of the spectrometer and for the very weak lines that occur within the spectral interval passed by the slit. Of course, errors in the assumed intensities of these very weak local lines lead to errors in the coefficients determined for the empirical continuum. However, it is unlikely that such errors are serious in very many of the narrow windows investigated. The intensities of these lines have been determined by a combination of theory and experiment prior to being included in the AFGL listings, and most are probably accurate to within a few percent. In most of the windows, these local lines contribute only a small fraction of the calculated absorption; therefore, errors in their assumed intensities are not expected to cause serious errors in the calculated values of transmittance.

This method of comparison also makes it possible to determine the empirical continuum without first determining the true values of the

absorption coefficient at all of the points within the interval passed by the spectral slit. The validity of the method depends on the assumption that $T(\text{emp})$, the transmittance of the empirical continuum, is constant over the spectral slitwidth. The results indicate that this assumption is valid, as we expect, since the empirical continuum is believed due to the extreme wings of the lines.

The coefficients eC^0 and K^0 are normalized to one atmosphere pressure of pure H_2O for self broadening and the same pressure of N_2 for N_2 broadening. Thus, the units for these coefficients include atm^{-1} along with the $\text{molecules}^{-1} \text{cm}^{-2}$. Inclusion of the atm^{-1} indicates that $-\ln T'$ for a given absorber thickness u (molecules cm^{-2}) is proportional to pressure. In accordance with the discussion in Section 1, this is true as long as all of the absorption at the particular wavenumber of interest is due to the wings of the lines. At the wavenumbers chosen for detailed study, this is essentially true for p_{N} less than one atmosphere and for the H_2O partial pressure p less than 0.2 atm. Thus, the assumed relationships are valid for applications to the earth's atmosphere. However, at higher pressures this simple relationship between $-\ln T'$ and pressure may not hold at some of the wavenumbers where the measurements have been made. This is true because some of the nearby lines are broad enough that their half widths are no longer small relative to the distances to the centers of the lines. (See Equation (1).)

Because of the finite spectral width of the slit used in the measurements, the spectrometer, when adjusted to the center of one of the windows of interest, may receive radiation at wavenumbers that include the centers of some of the nearby lines. Thus, we do not expect the measured $-\ln T$ to be exactly proportional to up (or up_{N}) at the centers of these windows. Comparing the experimental results as we did with the calculated values (including the convolved slitwidth) overcomes the problem of measuring the coefficient directly.

The method used also enables us to determine, with good reliability, the true transmittance T' , and thus the corrected value of K^0 , that would be observed with zero slitwidth. This corrected coefficient is given for self broadening by

$$K_S (\text{corrected}) = K_S (\text{calc}) + eC_S . \quad (17)$$

A corresponding equation applies to N_2 broadening.

As a check against possible errors in our method of reducing the data, we investigated the absorption in some of the windows by an alternate method that depends less on the accuracy of the assumed intensities of the local lines. Values of the empirical continuum coefficients obtained by this method agreed well with the others, thus adding confidence in the accuracy our method of accounting for the local lines and the finite slitwidth. In the alternate method, we obtained experimental spectra for pure H_2O samples at 2 or 3 different pressures, and plotted the quantity $(-1/u) \ln T(\text{exp})$ vs p . In accordance with Equation (9) and the discussion

following the equation, the slope of the curve through the plotted points corresponds to the experimental coefficient $K(\text{wing})$ normalized to one atm pressure. From this experimental value, we then subtracted the calculated value of $K(\text{wing})$, normalized to one atm, to obtain eC_S .

Because the empirical coefficients are derived from the differences between two other coefficients, one experimental and one calculated, the percentage uncertainties in these empirical values may be larger than for either of the coefficients from which they are derived. Uncertainties in the experimental values vary widely from one portion of the spectrum to another. The largest uncertainties occur in the wings of the bands where the coefficients are so small that even the largest samples produce only a small amount of absorption. The uncertainty is also larger than normal for some of the narrow windows in the stronger part of the band where the local lines make a larger contribution, or where the observed transmittance depends strongly on the slitwidth.

The estimated uncertainty in the empirical coefficients listed in the following sections increases from approximately 10% or 15% in the main part of the band to as much as 50% in the wings of the band where the coefficients are small.

SELF BROADENING: 3000 - 4200 cm^{-1}

Figure 3 summarizes the results for self broadening at the centers of approximately 50 narrow windows throughout the strong vibration-rotation band. The calculated coefficients represented by the circles vary in value by approximately a factor of 1000 from the wings of the band to places in the central portion of the band within a few cm^{-1} of some of the very strong lines. These calculated values were determined, as explained above, by summing the contributions by all of the lines while assuming a simple Lorentz line shape.

As would be expected, the circles do not fall on a smooth curve because of the near-random distribution of the H_2O lines. Some of the wavenumbers may be within 2 or 3 cm^{-1} of lines that contribute much of the absorption, whereas others may not be within several cm^{-1} of a line that contributes significantly. Furthermore, the intensities of lines within an interval of several wavenumbers may vary widely. Note the two points at 3775.2 and 3791.04 cm^{-1} , which are much lower than the adjacent points. These wavenumbers occur in the window between the two branches of the band.

Corresponding values of the empirical continuum are represented in Figure 3 by triangles joined by lines. In the wings of the band, the empirical coefficients, eC_S , are typically from 3 to 6 times as large as the corresponding calculated coefficients. This ratio is smaller for the coefficients near the very strong lines around 3800 cm^{-1} . Each corrected coefficient is determined by summing the corresponding calculated coefficient and empirical continuum coefficient. Thus, the corrected coefficient represents the value that would be derived from a measurement made with infinite resolving power (zero slitwidth). In

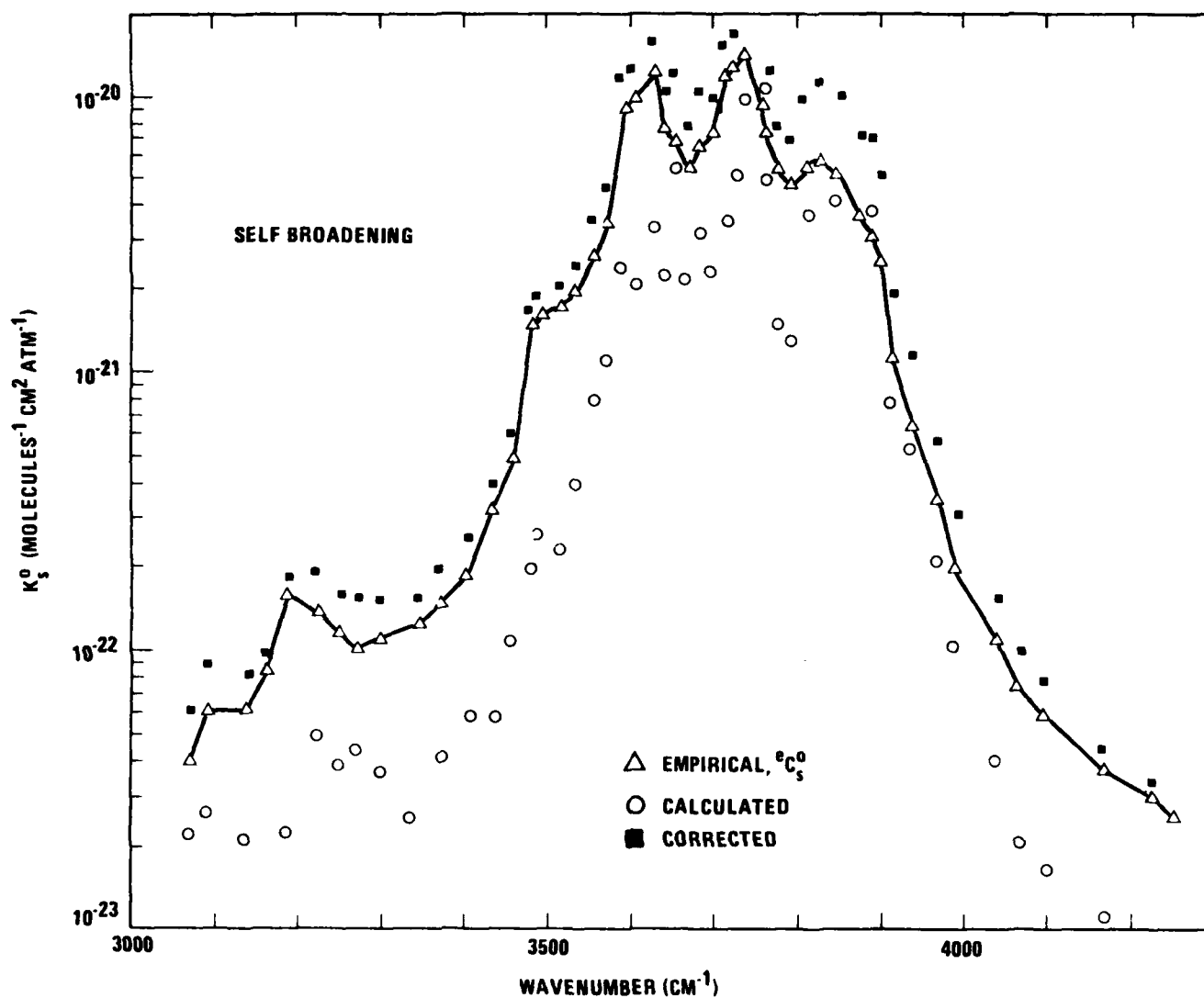


Figure 3: Spectral plots of the normalized absorption coefficients from 3000 to 4200 cm^{-1} for self broadening. The circles represent monochromatic transmittance values calculated from line parameters and the Lorentzian line shape. The triangles represent empirical values derived from the ratio of the experimental transmittance values to the monochromatic values calculated from line parameters and convolved with an instrument slit function (see Eqs. 14, 15). The corrected values (solid squares) are the sums of the empirical and calculated values (see Eq. 17). Temperature, 296K.

accordance with the above discussion, such a measurement must be made for a sample at a pressure sufficiently low that the half widths of any lines are much less than the distance from the point of measurement to the line centers. This condition is necessary for $-\ln(T)/u$ to be proportional to pressure, as is assumed in deriving the constants.

The left-hand portion of Table 1 summarizes the three sets of coefficients for self broadening plotted in Figure 3: the calculated, corrected and empirical continuum. The right-hand portion of the table includes comparable data from FASCODE, a widely used computer program developed at Air Force Geophysics Laboratory for line-by-line calculations. These data are discussed at the end of this sub-section.

The results shown here should not be mistakenly interpreted to mean that the actual absorption coefficients are 2 to 6 times as large as calculated values everywhere within the band. This is definitely not the case. Recall that the wavenumbers selected for the measurements were chosen at the centers of narrow windows within the band. Because of this method of selection, the absorption coefficients are much smaller than they are only a few cm^{-1} away where relatively strong lines are centered. Thus, at the wavenumbers studied, a large fraction of absorption is due to lines centered a few cm^{-1} , or further, away.

Lines centered in the wings of the band, approximately $3000 - 3500 \text{ cm}^{-1}$ and $4000 - 4200 \text{ cm}^{-1}$, are much weaker than those centered in the main part of the band. A calculated coefficient in the wing of the band typically contains a significant portion due to the lines centered from $1 - 10 \text{ cm}^{-1}$ away, but they also contain a large portion due to more distant lines. Although the lines centered in the main part of the band are very far from the narrow windows in the wings of the band, these lines are very strong and therefore make a sizeable contribution to the absorption in the narrow windows in the wings. Thus, a significant part of a coefficient in the wings may be due to lines centered more than 100 cm^{-1} away. By contrast, the narrow windows in the main part of the band are much nearer the very strong lines; therefore, only a small fraction of a calculated coefficient in this region is due to lines centered more than 10 or 20 cm^{-1} away.

We attribute the empirical continuum to a "super Lorentzian" shape of portions of the wings of the absorption lines. This shape can be described most easily in terms the following simple equation:

$$k = k_L \chi \quad (18)$$

where the correction factor χ is a function of $(\nu - \nu_0)$, and k_L represents the coefficient based on the Lorentz shape given by Equation (1). The line is said to be super-Lorentzian when $\chi > 1$, and sub-Lorentzian when $\chi < 1$. If $\chi > 1$, as we suggest, for the wings of the lines, it must be less than unity for a portion of the line near the center, in accordance with Equation (2). Our data do not provide any evidence either way about any slight deviations from the Lorentzian shape near the center or intermediate wings. However, it should be noted that

TABLE 1. COEFFICIENTS FOR SELF BROADENING

(Multiply all values by 10^{-24} molecules $^{-1}$ cm 2 atm $^{-1}$)

Wavenumber (cm $^{-1}$)	Present Work			FASCODE		
	Calc'd	Corrected	Emp'cal e $_C^O$ C $_S$	Calc'd	Cont'n'm (used)	Cont'n'm (suggested)
3072.48	22	66	44	50	35	51
3090.34	26	86	60	59	40	67
3138.24	21	81	60	47	34	68
3160.00	8	93	85	32	30	91
3188.90	22	182	160	50	35	167
3224.10	49	184	135	84	44	144
3250.40	40	155	115	77	47	125
3268.90	44	149	105	81	48	116
3301.62	36	146	110	75	50	121
3344.10	25	150	125	71	57	136
3372.16	42	192	150	99	73	166
3405.80	58	243	185	141	102	204
3454.70	108	578	470	254	179	503
3478.50	190	1645	1455	400	248	1493
3489.76	253	1818	1565	486	289	1621
3515.25	229	1954	1725	597	429	1786
3533.02	392	2342	1950	893	582	2031
3555.96	795	3445	2650	1454	849	2840
3572.02	1130	4480	3350	2049	1111	3542
3591.32	2345	11645	9300	3478	1569	9736
3604.70	2050	12350	10300	3592	1887	10645
3624.40	3330	15730	12400	5244	2413	12899
3640.60	2235	9935	7700	4569	2849	8215
3654.00	5530	12480	6950	8414	3238	7304
3664.20	2125	7675	5550	4956	3321	6040

TABLE 1. (Continued)

Wavenumber	Calc'd	Corrected	Emp'cal	Calc'd	Cont'n'm	Cont'n'm
3682.78	3150	10100	6950	6025	3433	7508
3698.64	2295	9495	7200	5344	3611	7762
3717.32	3420	15320	11900	6645	3916	12591
3739.62	9970	24720	14750	12572	4055	16203
3757.78	10820	19970	9150	12251	3928	11647
3761.80	4955	12355	7400	7983	3926	8298
3775.20	1460	6810	5350	4829	3843	5824
3791.04	1300	6225	4925	4411	3596	5410
3811.47	3700	9350	5650	7069	3870	6151
3829.00	5010	10860	5850	8560	4413	6713
3847.41	4145	9495	5350	7726	4142	5911
3877.63	3460	7010	3550	6190	3368	4188
3888.42	3835	6935	3100	6130	2744	3549
3895.85	2410	4910	2500	4468	2371	2813
3911.80	755	1875	1120	2289	1757	1343
3936.70	510	1140	630	1387	1006	759
3965.85	203	543	340	647	521	417
3987.30	103	298	195	392	333	239
4037.75	40	150	110	170	154	134
4068.60	21	96	75	109	105	92
4096.74	17	77	60	80	76	73
4167.98	11	41	30	38	36	39
4226.77	1	31	30	21	20	30

only a small fraction of the integral in Equation (2) is due to the wings where $|\nu - \nu_0|$ is greater than about 5 cm^{-1} , the approximate distance at which we suspect that χ becomes greater than unity. Thus χ would not need to differ much from unity for smaller values of $|\nu - \nu_0|$ in order for the integral of Equation (2) to be valid.

It could be informative to attempt the derivation of a modified shape for the lines that would predict the corrected values of the continuum coefficient listed in Table 1. Such a task is beyond the scope of the present study. In view of the uncertainties in the line parameters and the experimental data, it seems unlikely that a definitive line shape could be derived to fit all of the data. Since the cause of the deviation of the shape is not understood, it might not be realistic to assume that all of the lines have the same shape.

Although it would be difficult, if not impossible, to derive a single function $\chi(\nu - \nu_0)$ that would result in agreement between calculated and observed values, certain qualitative characteristics of the shape seem consistent. Results of the present study and previous studies of this type indicate that χ for self-broadened lines becomes greater than unity at $|\nu - \nu_0|$ equal to about 5 or 10 cm^{-1} . The value of χ then probably increases with increasing $|\nu - \nu_0|$ until it approaches 10 or more at $|\nu - \nu_0| = 100 \text{ cm}^{-1}$. Recall that the ratios of some of the corrected coefficients to the calculated ones in the wing of the band below 3500 cm^{-1} are between 10:1 and 5:1. For values of $|\nu - \nu_0|$ as large as 100, the more complex line shapes discussed in references 5 and 6 should replace the overly simple Lorentz shape given in Equation (1), and empirical changes should be made to the more appropriate shape.

The method used to determine the empirical continuum coefficient from data obtained with spectral slits as wide as 1 cm^{-1} is based on the assumption that the continuum is constant over this interval. We have checked this assumption in a few different spectral intervals, and the results indicate that the assumption is valid. For example, we consider the interval from approximately 3680 to 3684 cm^{-1} shown in the upper panel of Figure 2.

At 3682.8 cm^{-1} , near the peak transmittance, the experimental transmittance is 0.400, and the calculated transmittance, including the slit function, is 0.710. Dividing the first of these values by the latter, we find $T(\text{emp})$, the transmittance of the empirical continuum, to be 0.563. Following the same procedure, we find $T(\text{emp})$ to be 0.570 at 3679.5 and 0.556 at 3684.5 cm^{-1} , the two wavenumbers where the transmittances are at minima. In addition, we found the average $T(\text{emp})$ for the entire interval $3679.5 - 3684.5 \text{ cm}^{-1}$ to be 0.546. All of these values for $T(\text{emp})$ agree within expected experimental error; thus, we conclude that this quantity is essentially constant over the 5 cm^{-1} wide interval.

We made similar checks on the empirical continuum at different places within several other intervals. In all cases, the empirical continuum

appeared essentially constant, within experimental uncertainty, over intervals 2 - 5 cm^{-1} wide.

The two absorption lines centered near 3679.5 and 3684.5 cm^{-1} are strong enough to be opaque near their centers for the sample represented in Figure 2. However, these two lines contribute only a small fraction of the continuum absorption near 3682.8 cm^{-1} . Most of this continuum arises from much stronger lines centered outside of the interval shown in the figure.

Our simple suggested model of a super-Lorentzian line shape would lead to an empirical continuum that changes very little over a distance of a few cm^{-1} . As explained above, we believe that the empirical continuum exists because x in Equation (18) is greater than unity for $|\nu - \nu_0|$ greater than some value, approximately 5 to 10 cm^{-1} . It is likely that x increases gradually with increasing $|\nu - \nu_0|$; it may reach a maximum and start decreasing, but the changes are expected to be gradual. Thus, the sum of the contributions of many lines would change gradually.

Comparison With FASCODE Scientists at AFGL have developed a very efficient program to compute absorption coefficients from the AFGL line parameters⁴. This widely used program called FASCODE⁶ does not sum the contributions by all of the lines in the inefficient manner employed for the calculations discussed above. Instead, it calculates, point by point, the sum of the contributions of the nearby lines, those within approximately 25 cm^{-1} . A continuum is then added to this result to account for the more distant lines and for empirically determined deviations from the simple theoretical line shape.

The continuum now used as part of the FASCODE program for the spectral region covered by this report was based on empirical line shapes derived from a combination of theory and experimental results from lower wavenumbers. The new data presented in this report provide a means of checking the accuracy of the FASCODE continuum. Note that the FASCODE continuum does not represent the same physical quantity as the empirical continuum represented in Figure 3 and Table 1. Our empirical continuum represents the difference between experimental results and theoretical results based on all of the lines, with the assumption that the line shapes are given by Equation (1). On the other hand, the FASCODE continuum was intentionally made to include the contributions due to distant (further than approximately 25 cm^{-1}) lines as well as empirical corrections for the super-Lorentzian line shapes observed at lower wavenumbers.

Figure 4 compares the corrected coefficients, based on our self broadening data, with the corresponding values calculated by FASCODE. These quantities are directly comparable because they relate to the total coefficient, which includes contributions due to nearby lines and continuum. The corrected coefficients representing our data in Figure 4 are the same as those in Figure 3. We note that in most cases our corrected values are greater than the values based on FASCODE thus

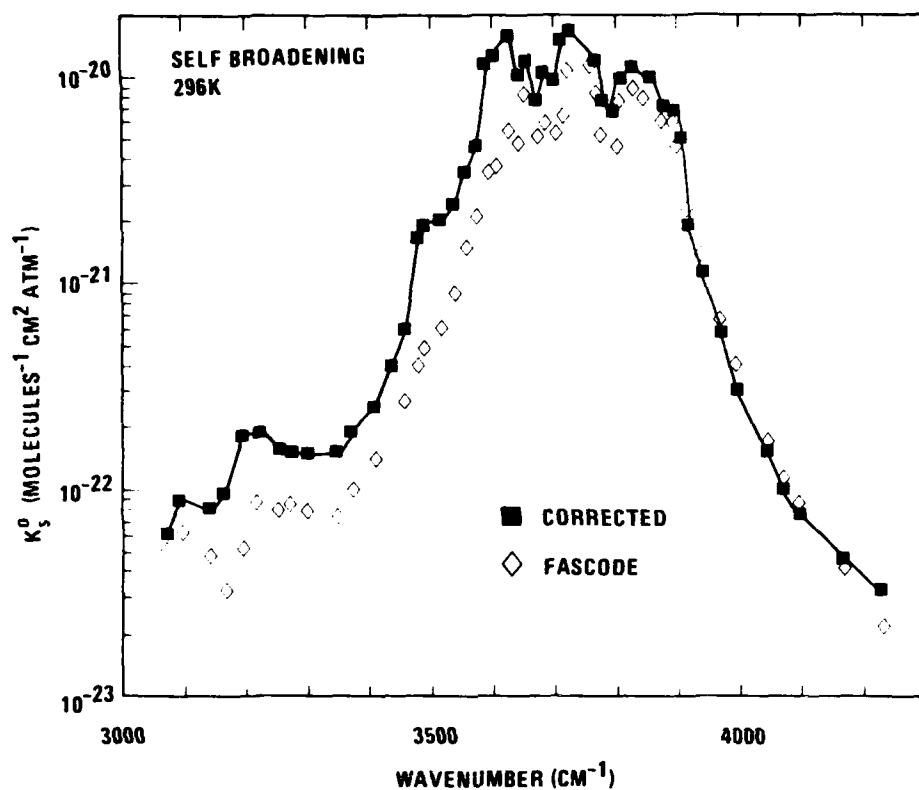


Figure 4: Corrected absorption coefficients for self broadening, from Fig. 3 and Table 1, compared with the coefficients calculated from FASCODE (see Table 1), including contributions from FASCODE local lines and continuum (see reference 6). Temperature, 296K.

indicating that the FASCODE continuum should be increased to improve the agreement with experimental results.

The right-hand portion of Table 1 gives more detailed results of the FASCODE calculations, and provides a point-by-point comparison with our results. Columns 3 and 5 contain the quantities plotted in Figure 4. Column 6 shows the portions of each coefficient due to the FASCODE continuum; the remainder of the coefficient in column 5 is due to the nearby lines.

In almost all cases, the calculated values for the total coefficient based on FASCODE (column 5) are smaller than the corresponding experimental values in column 3 but larger than our calculated values in column 2. The latter of these two results is due to the super-Lorentzian line shape assumed by the authors of FASCODE in determining their continuum. Our corrected coefficients indicate that the lines are more super-Lorentzian than the FASCODE authors assumed, and that the continuum should be increased. The values suggested for the continuum are listed in the last column of Table 1. Usage of these suggested values instead of those now used would bring FASCODE calculations into agreement with our experimental results.

N₂ BROADENING: 3000 - 4100 cm⁻¹

Figure 5a and the left-hand portion of Table 2 summarize the results of the investigation of N₂ broadening in most of the narrow windows included in the study of self broadening. As in Figure 3, the circles in Figure 5a represent the calculated continuum coefficients based on the simple Lorentz shape. The normalized halfwidths of the lines used for N₂ broadening are the ones in the AFGL listing. In accordance with the self-broadening coefficient defined by Equation (7), these half widths are one-fifth as large as the corresponding ones for self-broadening. Therefore, the calculated continuum coefficients for N₂ broadening are smaller by the same ratio.

The overall shapes of the empirical continuum curves for self broadening and N₂ broadening are similar. However, the values for N₂ broadening are typically less than one-tenth the corresponding values for self broadening. The figures and Table 2 also show that the ratios of the empirical continuum coefficients to the calculated coefficients are much smaller for N₂ broadening than for self broadening. Also, as for the self broadening, this ratio is less near the very strong lines in the main part of the band than it is in the wings.

The empirical continuum for N₂ broadening can also be explained in terms of super-Lorentzian lines. The factor χ in Equation (18) probably becomes greater than unity at $|\nu - \nu_0|$ equal to approximately 10, and continues increasing until $|\nu - \nu_0|$ is greater than 100 cm⁻¹. Measurements¹⁻³ in the major atmospheric windows indicate that χ for N₂ broadening decreases after reaching some maximum value and becomes less than unity for very large $|\nu - \nu_0|$. The maximum value of χ is apparently much greater for self-broadening than for N₂ broadening.

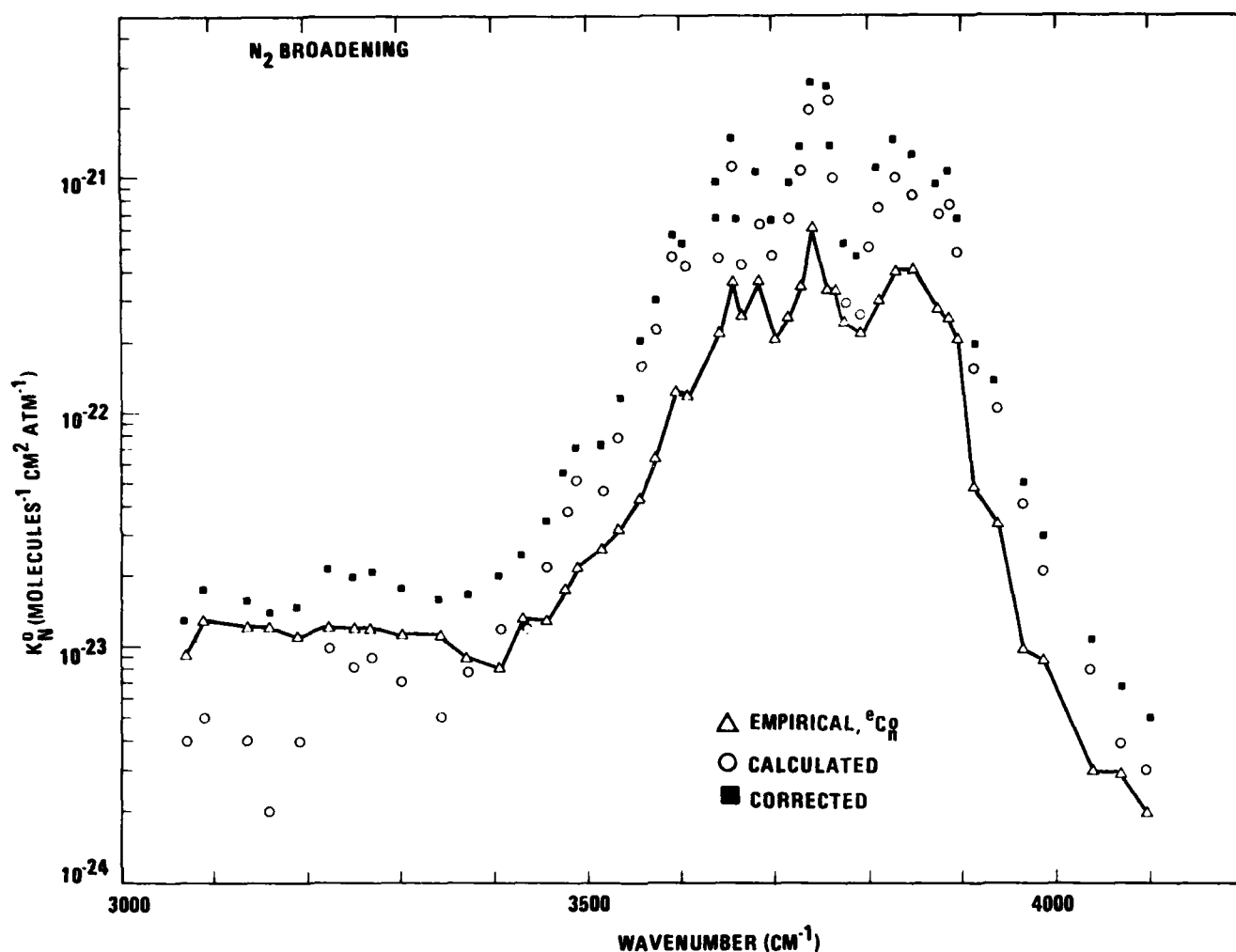


Figure 5a: Spectral plots of the normalized absorption coefficients from 3000 to 4200 cm^{-1} for N_2 broadening. The circles represent monochromatic transmittance values calculated from line parameters and the Lorentzian line shape. The triangles represent empirical values derived from the ratio of the experimental transmittance values to the monochromatic values calculated from line parameters and convolved with an instrument slit function (see Eqs. 14, 15). The corrected values (solid squares) are the sums of the empirical and calculated values (see Eq. 17). Temperature, 296K. (Compare with Figure 3.)

Comparison With FASCODE. Figure 5b and the right-hand portion of Table 2 provide comparisons of our results for N_2 broadening with calculations based on FASCODE. Each column of Table 2 corresponds to the same column for self broadening in Table 1.

The calculated values for N_2 broadening based on FASCODE generally agree with our experimental results much better than do the corresponding self broadening data in Table 1 and Figure 5a. At many of the wavenumbers, the discrepancy is less than the experimental uncertainty.

EMPIRICAL CONTINUUM: 1300 - 2200 cm^{-1}

Like the 3000 - 4200 cm^{-1} interval, the 1300 - 2200 cm^{-1} region contains many very strong lines that make up a vibration-rotation band of H_2O vapor. This region is bounded on both sides by wide windows, and essentially all of the absorption arises from lines centered within the spectral interval. In Reference 1, we reported on a study of the continuum absorption in several narrow windows within this band. The method of analysis was slightly different from the method employed in the present study of the 3000 - 4200 cm^{-1} region, but the objectives were the same. Because of the strong similarity in the results we have included three figures from the previous report for comparison with the data for the 3000 - 4200 cm^{-1} region.

Figure 6, which corresponds closely to Figure 3 for the higher-wavenumber region, shows that the experimental values for the self-broadening continuum coefficient are greater than the calculated coefficients. The general contour of the empirical continuum curve follows the smooth contour of the absorption band. The maxima that occur at approximately 1530 cm^{-1} and 1659 cm^{-1} are near the peaks of the two branches of the band, and the minimum near 1580 cm^{-1} is close to the window in the center of the band.

A composite of several curves of empirical continuum from the previous work are shown in Figure 7 for both self broadening and N_2 broadening. The overall shape of the curves for N_2 broadening is very similar to that for self broadening, but the largest N_2 broadening coefficients are less than one-tenth as large as the corresponding values for self broadening. Both of these results are very consistent with the findings in the 3000 - 4200 cm^{-1} region.

Figure 7 also illustrates an obvious strong decrease in the continuum coefficients with increasing temperature, another result that is consistent with the continuum in other spectral regions^{1-3,8}.

8. D. E. Burch and R. L. Alt, AFGL-TR-84-0128, ADA 147391 Scientific Report No. 1, AFGL Contract No. F19628-81-C-0118 (1984).

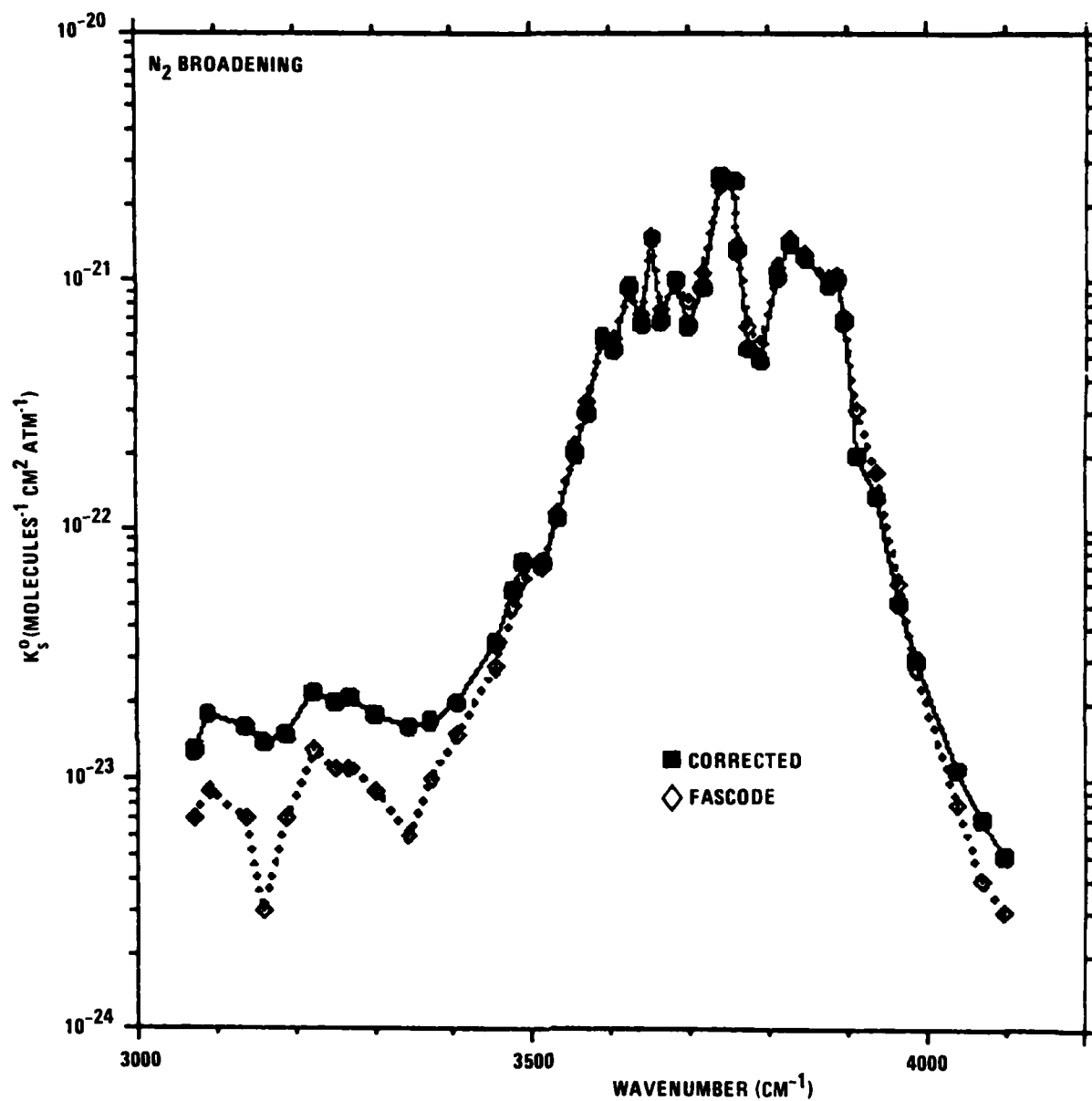


Figure 5b: Corrected absorption coefficients for N_2 broadening, from Fig. 5a and Table 2, compared with the coefficients calculated from FASCODE (see Table 2), including contributions from FASCODE local lines and continuum (see reference 6). Temperature, 296K. (Compare with Figure 4.)

TABLE 2. COEFFICIENTS FOR NITROGEN BROADENING
(Multiply all values by 10^{-24} molecules $^{-1}$ cm 2 atm $^{-1}$)

Wavenumber (cm $^{-1}$)	Present Work			FASCODE		
	Calc'd	Corrected	Emp'cal e_{CN}	Calc'd	Cont'n'm (used)	Cont'n'm (suggested)
3072.48	4	13	9	7	4	10
3090.34	5	18	13	9	5	14
3138.24	4	16	12	7	4	13
3160.00	2	14	12	3	3	14
3188.90	4	15	11	7	4	12
3224.10	10	22	12	13	5	14
3250.40	8	20	12	11	5	14
3268.90	9	21	12	11	5	15
3301.62	7	18	11	9	4	13
3344.10	5	16	11	6	4	14
3372.16	8	17	9	10	4	11
3405.80	12	20	8	15	6	11
3454.70	22	35	13	28	11	18
3478.50	38	56	18	49	17	24
3489.76	51	73	22	63	21	31
3515.25	46	73	27	69	35	39
3533.02	79	111	32	116	52	47
3555.96	159	202	43	215	83	70
3572.02	226	292	66	326	116	82
3591.32	469	594	125	586	177	185
3604.70	410	528	118	581	221	168
3624.40	665	951	286	899	296	348
3640.60	448	669	221	732	355	292
3654.00	1105	1472	367	1485	409	396
3664.20	425	686	261	763	421	344

TABLE 2. (Continued)

Wavenumber	Calc'd	Corrected	Emp'cal	Calc'd	Cont'n'm	Cont'n'm
3682.78	630	1007	377	964	430	473
3698.64	459	662	203	815	445	292
3717.32	685	936	251	1077	485	344
3739.62	1995	2631	636	2412	520	739
3757.78	2165	2504	339	2508	493	489
3761.80	990	1330	340	1383	488	435
3775.20	292	533	241	660	460	333
3791.04	260	474	214	559	428	343
3811.47	740	1040	300	1132	483	391
3829.00	1000	1405	405	1468	571	508
3847.41	830	1236	406	1271	542	507
3877.63	690	967	277	1033	427	361
3888.42	765	1018	253	1038	336	316
3895.85	482	691	209	710	282	263
3911.80	151	199	48	304	195	90
3936.70	102	135	33	171	92	56
3965.85	41	51	10	61	34	24
3987.30	21	30	9	28	15	17
4037.75	8	11	3	8	4	7
4068.60	4	7	3	4	3	6
4096.74	3	5	2	3	2	4

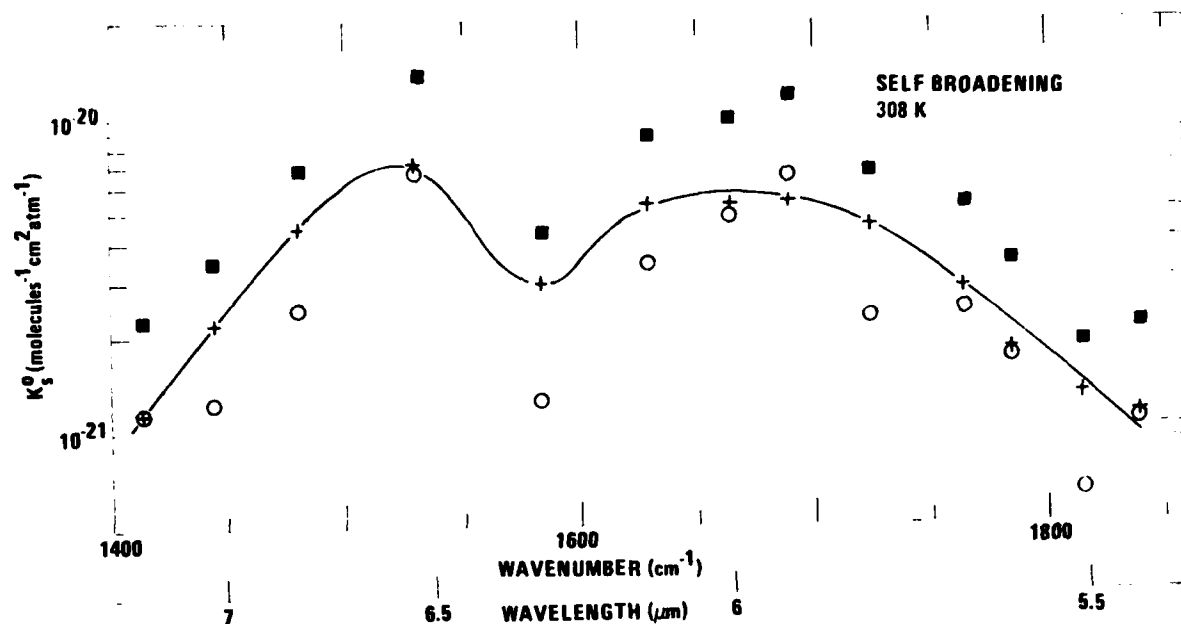


Figure 6: Spectral plots of the normalized absorption coefficients from 1300 to 1800 cm⁻¹ for pure H₂O. The empirical continuum curve is drawn through the +’s, which represent the differences between the experimental values (solid squares) and the calculated values (circles) based on the line parameters. Temperature, 308K. (from Ref. 1).

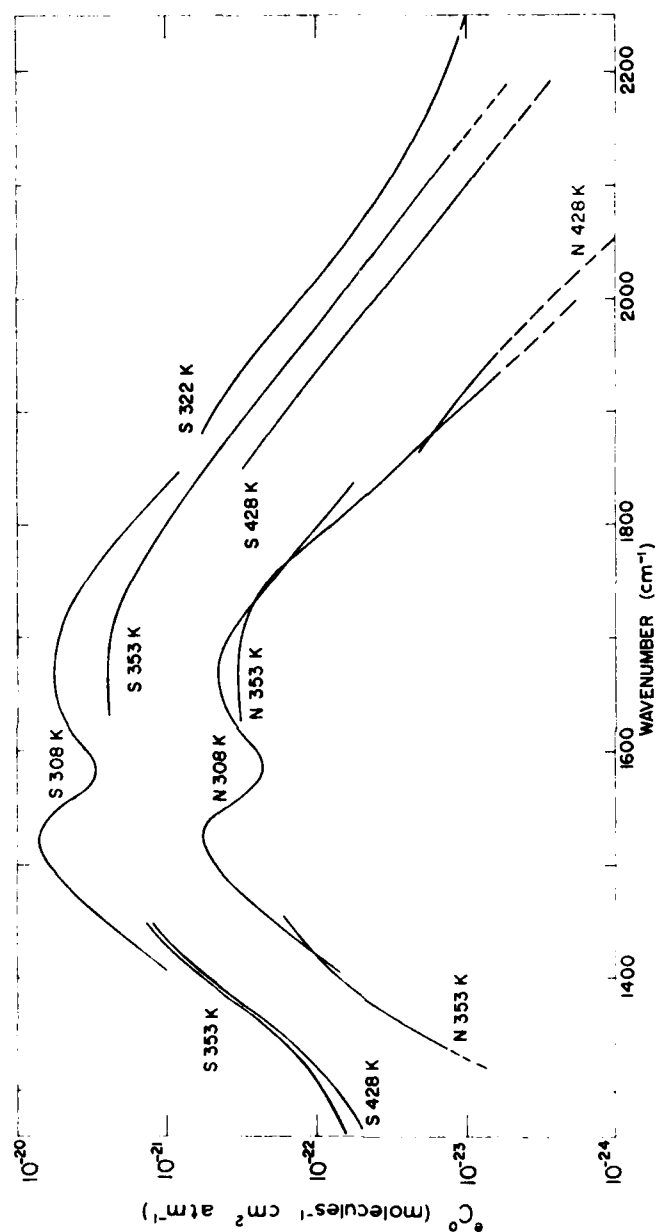


Figure 7: Composite of spectral curves from 1300 to 2200 cm $^{-1}$ of the empirical continuum at various temperatures. S, self broadening; and N, N $_2$ broadening.

A quantitative interpretation of the obvious decrease in the coefficients with increasing temperature is complicated by the shift in the intensities of the lines. As the temperature increases, the lines in the wings of the band increase in intensity at the expense of the lines closer to the band center (near 1595 cm^{-1}). This shift causes a coefficient in the wings of the band to be higher at high temperatures than it would be if the lines remained constant in intensity while changing in shape and width.

SPECTRAL BAND CONTOURS OF LIQUID, VAPOR, AND EMPIRICAL CONTINUUM

Some research workers have attributed the excess absorption by H_2O in different spectral regions to clusters of H_2O molecules that take on many of the absorption characteristics of liquid water. To get an indication of the validity of this hypothesis we have compared the spectra of the empirical continuum with those of liquid water. The comparisons are shown in Figures 8 for the $3000 - 4200\text{ cm}^{-1}$ region, and in Figure 9 for the previous work in the $1300 - 2200\text{ cm}^{-1}$ region. Each of these figures also contains a curve (V) that represents the smoothed contours of the vibration-rotation band of the H_2O vapor.

The curve labeled (V) in Figure 8 was obtained by summing the intensities of all the absorption lines in each 25 cm^{-1} wide interval. The value to be plotted for a given interval was derived by giving full weight to the sum for that interval and half weight to each adjacent interval. These weighted values were then plotted to form the basis for the curve. A similar method was used to derive the corresponding curve for Figure 9. These two curves labeled (V) show the general contour of the band without the excessive structure that would exist without the averaging.

The similarity between the curves for vapor and empirical continuum in Figure 9 is remarkable. Both curves show maxima at the peaks of the P- and R- branches and a minimum near the center of the band. In the original report¹, we interpreted this similarity as evidence that the empirical continuum is associated with the vibration-rotation lines. There is little similarity between the empirical continuum curve and the curve labeled L, which represents the absorption coefficient of liquid water. Thus, it seems unlikely that the excess absorption represented by the empirical continuum is due to liquid-like clusters.

The similarity between the vapor curve and the empirical continuum curve in Figure 8 is somewhat less than it is in Figure 9. Both curves in Figure 8 are highest in the $300 - 500\text{ cm}^{-1}$ wide region that contains the strongest lines, and both show a minimum at approximately 3701 cm^{-1} near the band center. However, the empirical continuum also contains some structure not present in the vapor curve between 3600 and 3800 cm^{-1} , a region that includes several very strong lines. Structure also appears in this spectral region in the empirical continuum curve for N_2 broadening in Figure 5. We have not attempted to determine quantitatively the cause

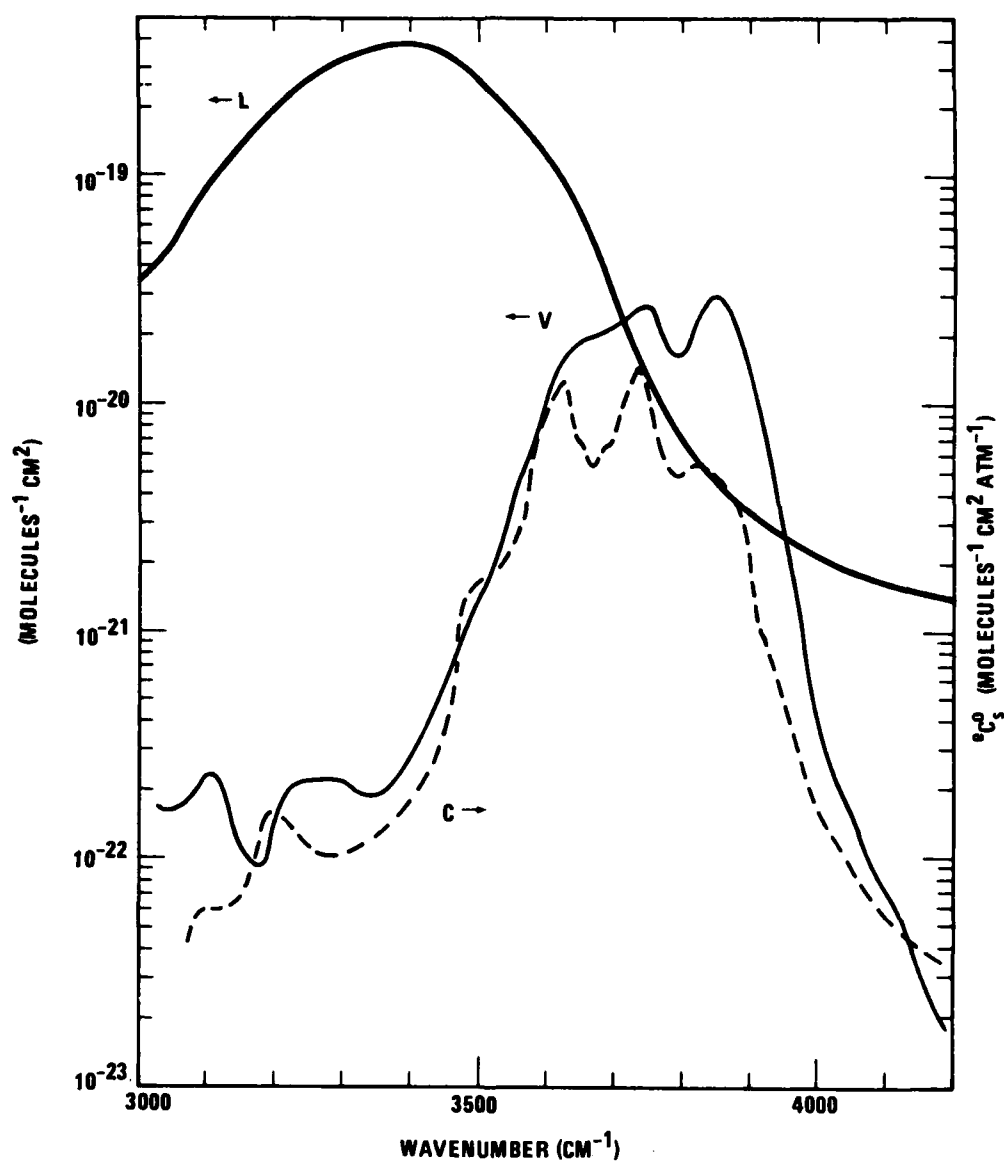


Figure 8: Comparison of the spectral curves between 3000 and 4200 cm^{-1} of the empirical continuum for self broadening (C), the absorption coefficient of liquid water (L), and the average intensities of the H_2O vapor lines (V). The arrows point to the appropriate scales for the curves.

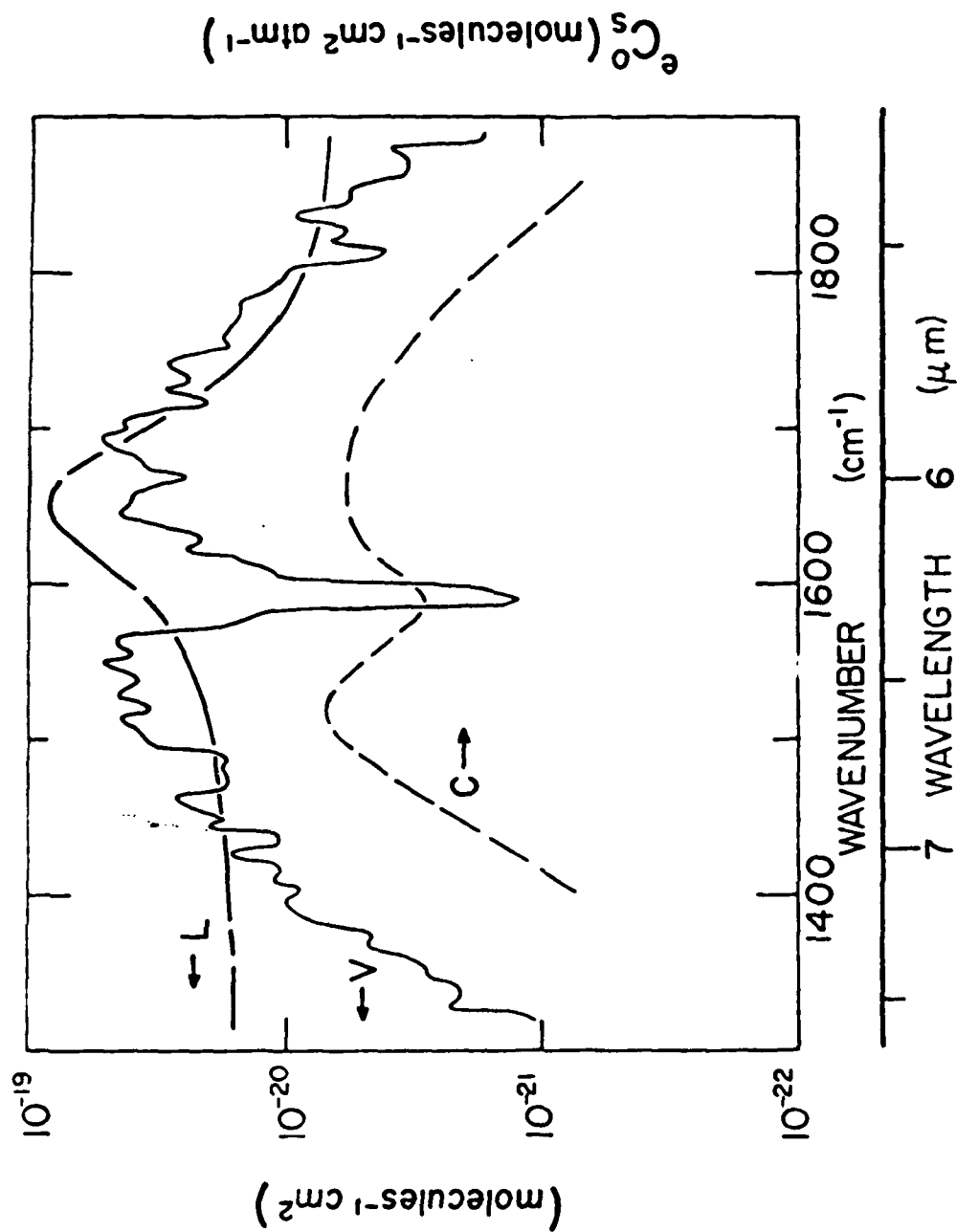


Figure 9: Comparison of the spectral curves between 1350 and 1850 cm $^{-1}$ of the empirical continuum for self broadening (C), the absorption coefficient of liquid water (L), and the average intensities of the H $_2$ O vapor lines (V).

of this structure, which is uncharacteristic of empirical continuum curves in other spectral regions¹.

The similarities in the shapes of curves C and V in Figures 8 and 9 suggest that the excess absorption represented by the empirical continuum is associated directly with both the rotational transitions and the vibrational transition involved in the band. It seems unlikely that the empirical continuum would display the spectral characteristics it does if it were due to a completely different process that involves dimers made up of two bound H_2O molecules rotating as semi-rigid rotators or vibrating in a mode that involves relative motion between the two molecules. If the excess absorption is due to dimers, as been suggested by other research workers, the binding is apparently such that each H_2O molecule forming a dimer is still free to vibrate and rotate similar to the way it does in the normal monomer state. Significant shifts would be expected in the vibrational and rotational frequencies if the absorption were due to dimers.

The very significant effect of the N_2 broadening represented in Figure 5a and 7 suggests further that the excess absorption is associated directly with the vibration-rotation band rather than with dimers or clusters. Continuum absorption by dimers or clusters is expected to be essentially independent of the presence of nonabsorbing N_2 . Thus, it seems likely that much of the excess absorption is due to the extreme wings of individual absorption lines that absorb more than is predicted by any of the widely used theoretical line shapes.

SECTION 4

PREVIOUS REPORTS AND PAPERS UNDER PRESENT CONTRACT

The present contract has dealt almost exclusively with the infrared continuum absorption by H_2O vapor. Essentially all of the results of the experimental investigation are included in this report and a Scientific Report published in 1984.

The results of some of the work was also presented in oral papers at the 1982 and 1983 Annual Review Conferences at AFGL.

The reference and the abstract of the Scientific Report are as follows:

D. E. Burch and R. L. Alt, AFGL-TR-84-0128
Scientific Report No. 1, AFGL Contract
F19628-81-C-0118 (1984)

New laboratory measurements have been made of the H_2O continuum absorption at several wavenumbers within the $700\text{-}1200\text{ cm}^{-1}$ and $2400\text{-}2800\text{ cm}^{-1}$ regions. Samples of both pure H_2O and $\text{H}_2\text{O} + \text{N}_2$ have been studied in a multiple-pass absorption cell at path lengths up to more than 800 meters. Data for samples of pure H_2O at reduced temperature (284 K) indicate that the self-broadening coefficients increase with decreasing temperatures at about the rate predicted by extrapolating from previous data on samples at elevated temperatures. Coefficients for N_2 broadening have been measured in both windows, and the results compared with previous work. The results have been compared with the data base for the well-known transmission computer code LOWTRAN 6.

SECTION 5

REFERENCES

1. D. E. Burch, Continuum Absorption by H_2O , AFGL-TR-81-0300, ADA112264, Final Report, AFGL Contract No. F19628-79-C-0041 (1982).
2. D. E. Burch and D. A. Gryvnak, Continuum Absorption by H_2O Vapor in Atmospheric Water Vapor (A. Deepak, T. D. Wilkerson and L. H. Ruhnke, eds.), Academic Press, New York (1980).
3. D. E. Burch, SPIE Proceedings 277, 28 (1981).
4. R. A. McClatchey, W. S. Benedict, S. A. Clough, D. E. Burch, R. F. Calfee, K. Fox, L. S. Rothman, and J. S. Garing, AFCRL Atmospheric Absorption Line Parameters Compilation, AFCRL-TR-73-0096, U. S. Air Force (1973). (Available from NTIS), AD762904.
5. S. A. Clough, F. X. Kneizys, R. Davies, R. Gamache, and R. Tipping, Theoretical Line Shape for H_2O Vapor: Application to Continuum, in Atmospheric Water Vapor (A. Deepak, T. D. Wilkerson, and L. H. Ruhnke, eds.), Academic Press, New York (1980).
6. S. A. Clough, F. X. Kneizys, L. S. Rothman, W. O. Gallery, Atmospheric Spectral Transmittance and Radiance: FASCOD1B, SPIE Proceedings 277, (1981).
7. D. E. Burch, D. A. Gryvnak, R. R. Patty, Scientific Report, Contract No. 3560(00), ARPA Order No. 273/11-7-63 (1965).
8. D. E. Burch and R. L. Alt, Continuum Absorption by H_2O in the $700-1200\text{ cm}^{-1}$ and $2400-2800\text{ cm}^{-1}$ Windows, AFGL-TR-84-0128, ADA147391, Scientific Report No. 1, AFGL Contract No. F19628-81-C-0118 (1984).

END
FILMED

5-86

DTIC